NANO LETTERS

2008
Vol. 8, No. 8
2452-2457

Chiral Shells and Achiral Cores in CdS Quantum Dots

Simon D. Elliott*

Tyndall National Institute, Lee Maltings, Cork, Ireland

Mícheál P. Moloney and Yurii K. Gun'ko†

CRANN, School of Chemistry, TCD, Dublin, Ireland

Received May 21, 2008; Revised Manuscript Received June 27, 2008

ABSTRACT

We report and explain circular dichroism in semiconductor quantum dots. CdS nanocrystals capped with penicillamine enantiomers were prepared and found to be both highly luminescent and optically active. No new features in circular dichroism were observed as the nanocrystal grew larger. Density functional calculations reveal that penicillamine strongly distorts surface Cd, transmitting an enantiomeric structure to the surface layers and associated electronic states. The quantum dot core is found to remain undistorted and achiral.

Because of quantum confinement effects due to their nanometer size, fluorescent semiconductor nanocrystals or quantum dots (QDs) have remarkable optical, physical and chemical properties, which differ markedly from the bulk material.[1–9] The ability to tune their optical properties, combined with the ease of surface modification has led to their proposed application in inter alia light emitting devices, fluorescent sensors and bioassays.[2–4,10–12]

Chirality is one of the most important factors of molecular recognition and therefore development of chiral luminescent nanosized probes would provide very useful tools for both chemistry and biology. Although there have been some recent publications on the preparation of chiral gold [13,14] and silver[15,16] nanoparticles, there has been very little work on chiral light emitting particles, with only one type of chiral QDs having been reported so far.[17]

In this communication we describe the preparation, characterization and modeling of green-white or blue-white emitting, optically active, water-soluble chiral CdS QDs, which we believe should have a broad range of potential applications. The CdS QDs are stabilized by the chiral ligand penicillamine, (2*S*)-2-amino-3-methyl-3-sulfanylbutanoic acid, $C_5H_{11}O_2NS$, which is a known chelating agent for Cd and exists in *D*- and *L*- forms.[18] CdS quantum dots were prepared by first adding cadmium perchlorate to a basic solution of *D*-, *L*- or *rac*-penicillamine to form a chiral Cd-Pen complex. Addition of thioacetamide then created weakly luminescent CdS nanoclusters, which were microwaved to form highly luminescent chiral CdS nanoparticles of diameters in the ~5 nm range (Figure 1). The *D*- and *L*-functionalized dots demonstrate a chiral response from 380 nm (the onset of absorbance) to 200 nm. Because the particles are optically active from 200−360 nm, the chirality cannot be simply attributed to the Pen ligand and therefore the QDs themselves must be considered chiral.[17]

We relate this measured chiral response to the computed structure and degree of chirality of the QD. Schaaf and Whetten[14] propose three models that can account for a circular dichroism (CD) response from a metallic nanocluster with chiral ligands:

(i) the core of the nanoparticle is chiral (e.g., metals[13–16,19]);

(ii) the nanoparticle surface is chiral (analogous to the helical surfaces of some nanotubes);

(iii) only the adsorbate is chiral.

The central question is to what extent the enantiomeric structure of the ligand is transmitted to the atomic structure of the nanoparticle. In this study we test these three distinct possibilities. We develop a model of a CdS QD terminated with enantiomeric penicillamine ligands and compute its atomic and electronic structure using ab initio density functional theory. This is the first study of chiral QDs at this level of theory.

All types of CdS particles (capped with *D*-, *L*-, and *rac*-penicillamine) were highly luminescent after microwaving. The emission spectra (Figure 2) show broad peaks between 370 and 710 nm with the maximum wavelength at 495 ± 10 nm, indicating the presence of surface defects. The emission spectrum of each particle type was also found to be independent of excitation wavelength, consistent with uniform particle distribution. Although DLS (dynamic light scattering) shows particles with an average size of 2−3 nm,[17]

* Corresponding author. Tel: +353-21-4904392. Fax: +353-21-4270271. E-mail: simon.elliott@tyndall.ie.
† E-mail: igounko@tcd.ie.

10.1021/nl801453g CCC: $40.75
Published on Web 07/09/2008

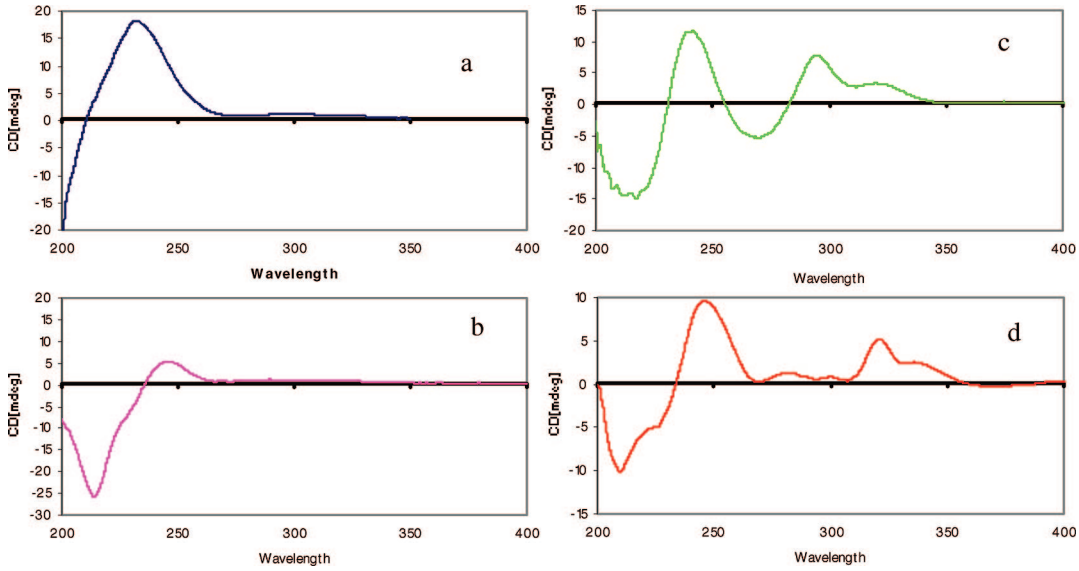

Figure 1. CD monitoring of the formation of *L*-CdS. (a) Free stabilizer (blue) as a band at ~230 nm. (b) Cd-penicillamine complex with a new band at ~210 nm (pink). (c) Clusters after addition of the thioacetamide before microwave treatment showing new bands from 290 to 320 nm (green). (d) CdS nanocrystals after microwave treatment with new bands from 320 to 390 nm (red). The spectra have been recorded using a JASCO J-810 Spectropolarimeter. Note: the final CdS samples were not purified in these monitoring experiments.

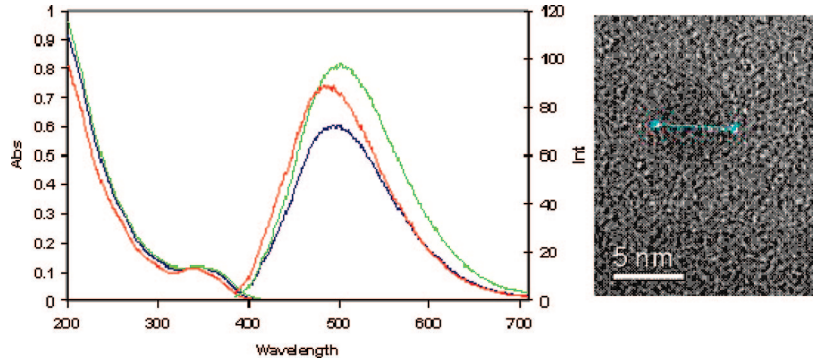

Figure 2. Left: optical spectra (UV−vis absorption <400 nm and emission >400 nm) of CdS nanocrystals stabilized with *D*-Pen (blue), *L*-Pen (green), and *rac*-Pen (red); excitation wavelength for all emission spectra is 365 nm. Right: HRTEM image of *D*-Pen CdS, showing a particle size of 5.6 nm with a lattice spacing of ~3.6 Å.

TEM indicates a larger average particle size of around 5 nm, which is more consistent with particles that possess an absorbance maximum at 340 nm. The maximum wavelength of the *rac* particles is the shortest, consistent with these particles being smaller. This may be attributed to the complementary nature of the *D*- and *L*-ligands, allowing for closer packing of the stabilizer on the surface of the *rac*-CdS.

All three types of CdS particles have absorption bands with maxima at 340 ± 5 nm. This band is assigned to the first excitonic (1sh−1se) transition.[17] The luminescence is considerably red-shifted in relation to the exciton peak and remains quite broad with a bandwidth half-maximum of 150 nm suggesting a defective surface.

CD studies of the particles gave particularly striking results. *D*- and *L*-penicillamine stabilized particles produced corresponding mirror image CD scans whereas the particles prepared with a *rac* mixture showed none. The CD observed for the particles is quite different from that of the free *D*- and *L*-penicillamine, which show, as expected, a near symmetrical image with maxima/minima at 234 ± 2 nm. However, the CD spectra of *D*- and *L*-QDs are more complex, with maxima/minima at 207 ± 3, 252 ± 2, 293 ± 3, 320 ± 2 and 345 ± 2 nm (Figure 1d). The opposite preference for left or right polarized light in the region of the CdS exciton bands is particularly intriguing. The presence of optical activity may be due to chirality induced in the QDs upon reaction, in a manner similar to that previously proposed for metallic nanoparticles.[13–15] The extent of the chirality is explored in this paper.

To understand the formation mechanism of these chiral QDs, UV and CD measurements were carried out at all stages of the particle preparation. Both *L*- and *D*- samples demonstrated similar behavior but showed bands of opposite chirality. According to these data, the process initially involves the formation of a Cd-penicillamine complex (maximum at 210 nm), which demonstrates a chiral response opposite to that of the starting stabilizer (Figure 1b). Then new species are formed after addition of the thioacetamide that result in the appearance of signals around 290 and 320

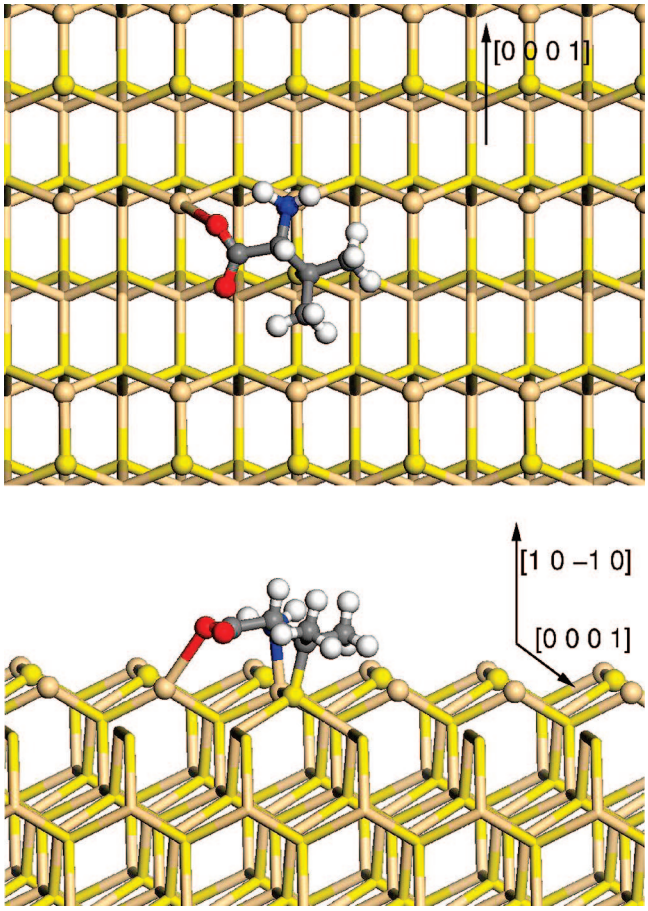

Figure 3. Top and side views of the proposed bonding of *D*-Pen to the $(10\bar{1}0)$ surface of wurtzite (Cd = brown, S = yellow, C = gray, O = red, N = blue, H = white, balls = topmost atoms). In the top view, horizontal rows of vertical CdS units are visible at the top and bottom of the figure, and surface S atoms have been removed from the middle row and one has been replaced by the S atom of *D*-Pen, so as to illustrate the bonding pattern found in this study.

nm in the CD spectra (Figure 1c). Most likely these are small CdS clusters to which penicillamine ligands are coordinated in a fashion similar to that proposed for other similar CdS systems[20,21] and modeled in this paper. Subsequent microwave irradiation causes the nucleation centers to grow into larger CdS nanocrystals, resulting in an increase in luminescence. This is accompanied by a red shift in the CdS band edge and corresponding CD signals between 320 and 390 nm respectively (Figure 1d).

The clusters were modeled as isolated molecules in vacuum. The ground-state electronic wave function of each cluster was calculated self-consistently within Kohn−Sham density functional theory (DFT) using the TURBOMOLE suite of quantum chemical programs.[22] A good tradeoff between accuracy and computational cost was obtained by using the B-P86 functional,[23] the RI-*J* approximation[24] and an atom-centered basis set of valence double-ζ with polarization quality [denoted SV(P)][25] with a 28-electron effective core potential on Cd.[26] Tests of this method[28] indicated that bond lengths were slightly overestimated (~5 pm), as is typical of DFT. All species were closed shell. Optimization of the cluster geometry was carried out on the DFT potential energy hypersurface.

We denote the neutral form of penicillamine as $PenH_2$, so that the dianion is Pen^{2-}, which is the probable charge state of the ligand in these experiments at pH = 11. Our calculations indicate that $-SC(CH_3)_2CH(NH_2)COO^-$ is the most stable dianionic structure in the gas phase. CdS can adopt either the wurtzite or the zinc-blende structure.[27] It is computed that wurtzite clusters show greater cohesive energy than zinc-blende clusters[28] and so we choose to focus on wurtzite-based QDs. In agreement with this selection, HR-TEM shows particles with lattice spacings of 3.6 Å (Figure 2), where the lattice spacing of bulk wurtzite in the *a* and *b* planes is 3.81 Å. In the hexagonal wurtzite structure (space group #186, $P6_3mc$), both S and Cd are tetrahedrally coordinated and stacked ABAB along the [0001] axis. The experimental Cd−S distance in the bulk is 2.52 Å.[29]

Initial structures for Pen-stabilized CdS QDs were obtained by cutting symmetrical clusters out of the bulk wurtzite structure, so as to expose the $(10\bar{1}0)$ and (0001) surfaces. CdS nanoparticles that have been computed in previous DFT studies[30] range in size up to $Cd_{16}S_{16}$ but are too small for this study. Because our interest is in distortion of the QD core, the smallest useful cluster is one based on Cd_{19} that contains a Cd_4S_4 core capable of distortion/twisting about [0001]. (We define core atoms as those that are not bound directly to surface Cd−S units). A coin-like disk is cut out of the bulk wurtzite structure, consisting of 19 parallel CdS units, each oriented along [0001], of which four are bulk-like (Cd_4S_4 core), six form intermediate (0001) planes and nine form three equivalent $\{10\bar{1}0\}$ faces around the outside of the QD. The (0001) plane was stabilized by H^+ (on S) and SH^- (on Cd), leaving the three $\{10\bar{1}0\}$ faces of the cluster for adsorption of Pen molecules.

The electronic structure of semiconductor clusters is notoriously difficult to compute accurately with DFT and similar ab initio methods.[28] "Bare" clusters are often unstable and convergent calculations are only possible if the surface is adequately stabilized by ligands in a realistic bonding configuration.[27] Unfortunately, experimental data on the structure of the ligand shell are rarely available, necessitating considerable computational trial and error in the nature and geometry of the ligands. Our first criterion is a closed-shell, well-converged electronic structure at the plausible starting geometry. Second, we require that molecular orbitals (MOs) of predominantly Cd:5s5p character be vacant and low-lying, and ligand valence MOs be occupied. In clusters with poorly saturated surfaces, the energetic ordering (and thus occupancy) of these MOs is erroneously reversed.

From this model, the bonding of *D*-Pen to $\{10\bar{1}0\}$ faces of the CdS QD was determined. In the perfect $(10\bar{1}0)$ surface, each topmost S atom caps three Cd, and so it is reasonable to assume that the S atoms of the Pen ligands also assume this position. The amine-N and carboxylate-O of Pen are also basic and each is available for coordination to Cd. Our tests on a variety of small clusters indicate that both N and O can bond to Cd, with a preference for Cd−N, and that neither atom bridges nor caps more than one Cd (although

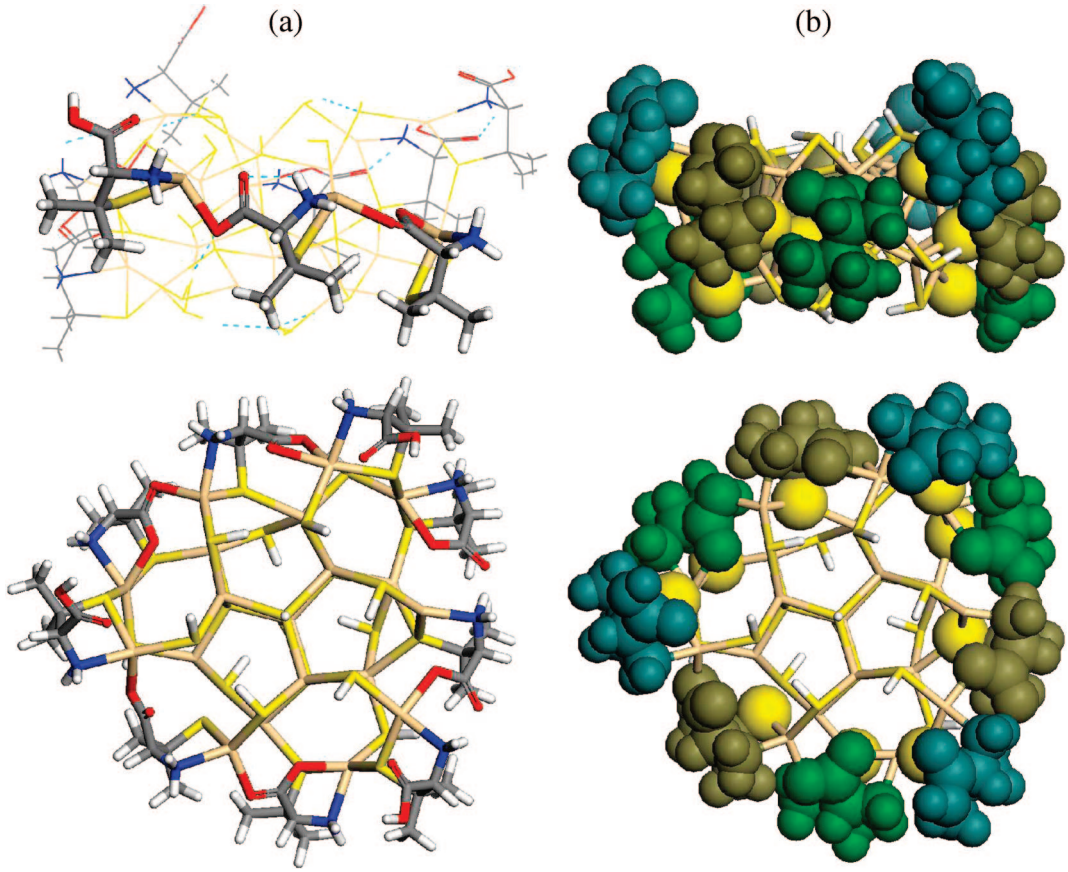

Figure 4. Top and side views of a $(10\bar{1}0)$ face of the optimized cluster model of QD: (a) stick representation with PenH-Pen-Pen bonding pattern along one face highlighted in the side view; (b) Pen ligands in space-filling representation, with non-S parts of each ligand colored differently. Note that *D*-Pen ligands form fragments of a left-handed helix about the QD core.

carboxylate may bridge two Cd via two O). This leads us to propose the bonding arrangement shown in Figure 3 for *D*-Pen on a perfect $(10\bar{1}0)$ surface. As the schematic shows, bonding via the carboxylate moiety to a fourth surface Cd atom is asymmetric and lifts the mirror symmetry of the surface. Thus, even without any distortion of the CdS substrate, the adsorption of *D*-Pen is expected to yield an enantiomeric monolayer of ligands. Our calculations aim to see how this affects underlying CdS in the case of a QD.

Our Cd_{19} model cluster has three identical $(10\bar{1}0)$ faces, each consisting of three [0001]-oriented CdS units. Using the bonding arrangement outlined above, we substitute *D*-Pen^{2-} for S^{2-} in these faces, so that each face is covered with a band of three Pen ligands, interlocked by H-bonding and coplanar in (0001). To obtain a reasonable electronic structure, it is necessary to saturate dangling $-COO^-$ at one edge of each face by adding H^+.[31] The cluster formula is thus $[Cd_{19}S_{17}H_{14}(D\text{-Pen})_6(D\text{-PenH})_3]^{3+}$. The geometry is fully optimized (first in C_3 symmetry and then without symmetry constraints) and the resulting structure is shown in Figure 4 and in the Supporting Information. This cluster shows a maximum diameter of about 21 Å, measured between outermost H's of the ligand shell, considerably smaller than the final QDs obtained experimentally.

Of the three *D*-Pen ligands bound to each face of the model cluster, the structure of the middle ligand is likely to be most representative of that occurring in the actual QD. The optimized structure shows the middle *D*-Pen coordinating to four Cd in much the same fashion as the starting structure (Figure 3), with distances Cd—N = 2.33 ± 0.06 Å, Cd—O = 2.36 ± 0.07 Å, 2.7 ± 0.4 Å and Cd—S = 2.58 ± 0.01 Å, 2.78 ± 0.02 Å, 2.9 ± 0.2 Å, all of which suggest strong binding of Pen to the QD surface. The N—Cd—S angle is 82.8 ± 0.4°. The margins of error reflect the slight differences between the three faces,[32] and are perhaps indicative of the geometrical variability that can be expected on imperfect surfaces of actual QDs.

On optimization, the band of three Pen ligands on each face are splayed apart by bulky CH_3 groups, increasing S—S distances within the $(10\bar{1}0)$ face (from 4.0[29] to 5.3 ± 0.9 Å) and causing rotation of the Cd—S units (tilting clockwise relative to [0001] by an average of 41°, standard deviation 14°). This is accommodated by expansion of the cluster perpendicular to the Pen-covered faces, with [0001] displacements of 0.5—1.0 Å by intermediate Cd and S atoms (i.e., atoms of the $Cd_6(SH)_{12}$ interface between the $(CdS)_9$ surface and the $Cd_3S_3Cd(SH)_2$ core). As noted above, the asymmetrical orientation of the ligand is dictated by the coordination of carboxylate-O to neighboring Cd (Figure 4a). The result is that $(D\text{-Pen})_3$ and the underlying Cd and S pack into a segment of left-handed helix on each face, as illustrated in Figure 4b. Clearly, in an *L*-Pen cluster, the ligands would tilt in the opposite sense (−41°) and form a right-handed helix.

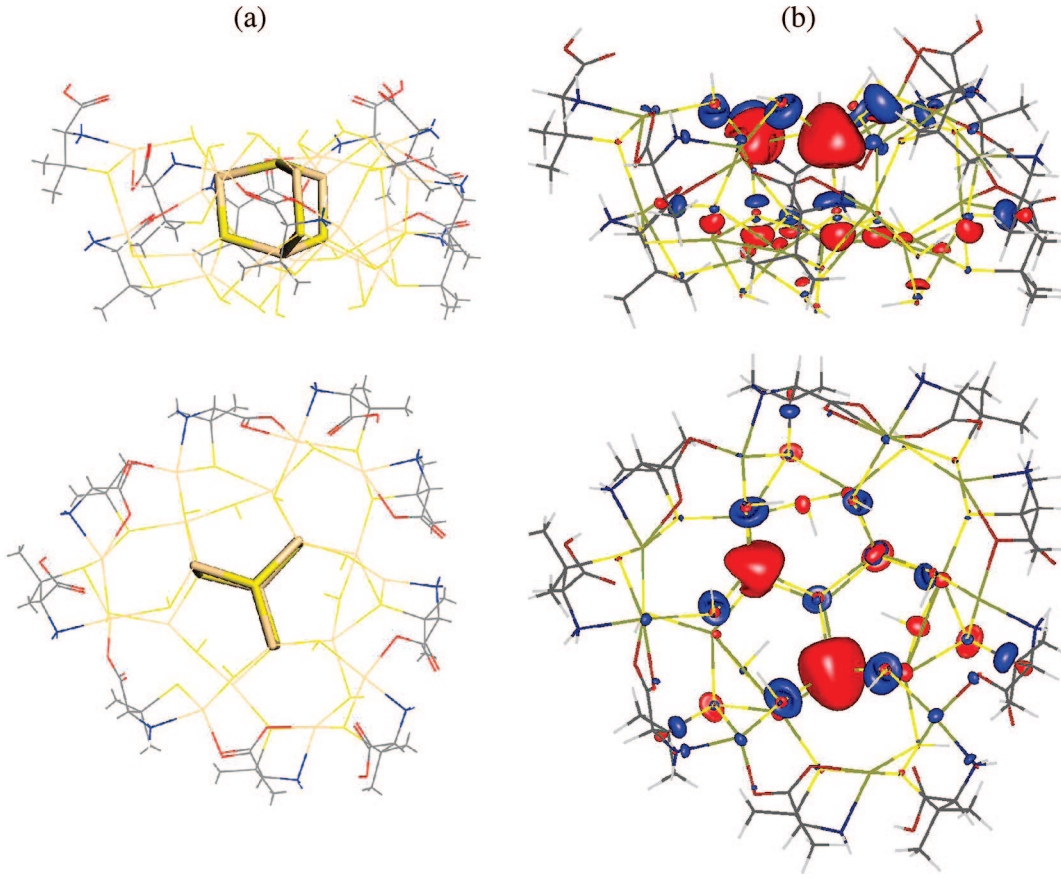

Figure 5. Top and side views of optimized cluster model of QD: (a) Cd_4S_4 core highlighted; (b) contour plot of empty LUMO+3 molecular orbital, which is mostly of Cd:5s character on the QD core.

This analysis suggests that three factors dictate the cluster geometry: (i) the Pen ligand is slightly bulkier than the space between adjacent Cd on $(10\bar{1}0)$; (ii) surface-Pen bonding is relatively strong and (iii) the Cd−S cluster structure is relatively flexible. As a result, interligand strain is transmitted to the outer layers of the CdS cluster, meaning that the chirality of the ligand shell is transmitted to these layers as well.

It is significant, however, to observe that the $Cd_3S_3Cd(SH)_2$ core of the QD cluster remains almost undistorted (Figure 5a): on optimization, the Cd−S units of the core tilt by only −5° to +2° relative to the perfect crystal, with Cd−S = 2.55 Å. The core therefore remains achiral, despite the chiral distortion of the surrounding layers. We propose that this finding may be generally true. The Pen-terminated CdS nanoparticles synthesized experimentally are larger and show a wider variety of cluster faces than considered here. Nevertheless, we suggest that the relative bond strengths of Pen, Cd and S are universal properties of the system and generally mean that the chirality of Pen is transmitted to the surface and subsurface layers, but that the QD core remains achiral.

Examination of the electronic structure of the computed cluster reveals that the three highest-lying occupied molecular orbitals (MOs) (not shown) are localized on surface S atoms at each corner of the QD (i.e., at the junction between $\{10\bar{1}0\}$ faces).[32] The three lowest-lying unoccupied levels (not shown) are of predominantly Cd character on highly distorted sublayer atoms near each corner. The corners in our model correspond to defects on a real QD surface. We stress that unoccupied MOs from a DFT calculation have no direct physical significance. Nevertheless, it is likely that these or similar chiral states on near-surface Cd are responsible for the long wavelength CD response of small QDs after treatment with thioacetamide (290−390 nm, Figure 1c) and for the defect-related luminescence of the larger QDs (Figure 2).

Above these lies an unoccupied MO of predominantly Cd:5s character on the Cd_4S_4 QD core (Figure 5b). Polarization of this MO is visible but is minor relative to the strong localization of the other frontier MOs. Optical absorption by the core is therefore predicted to be achiral. This is consistent with our experimental finding, where no new CD states emerge as the size of the QD core increases (Figure 1d). We conclude that optical absorption by the core is achiral, and absorption at surface defects is strongly influenced by the chirality of the surface layers.

To summarize, chiral semiconductor QDs have been synthesized and modeled with density functional theory. This has been achieved by stabilizing CdS nanocrystals with the chiral ligand penicillamine. Weakly luminescent QD nanoclusters were prepared by adding thioacetamide to a solution of cadmium perchlorate and *D*-, *L*- or *rac*-penicillamine. The QDs stabilized with *D*- and *L*-penicillamine show exactly opposite chiral optical responses. On the basis of calculated electronic states, we associate the longer-wavelength circular

dichroism with near-surface Cd atoms that are enantiomerically distorted by the penicillamine ligands. Subjecting the QDs to microwave irradiation yielded larger, highly luminescent QDs. The red-shift and broadness of the luminescence signal is indicative of a defective surface of the QD. The features in circular dichroism are red-shifted but no new features emerge, which is also consistent with growth of an achiral QD core, as predicted by our calculations.

Models of a typical QD surface show that the penicillamine ligand bonds via N and S to one surface-Cd, and introduces chirality via additional bonding of carboxylate to a neighboring Cd. The interaction between ligand and cluster is strong, as is the interaction between ligands on the surface, compared to the weaker CdS surface structure. The ligands thus pack into helical bands on the surface and strongly distort the outermost Cd atoms of the QD, transmitting an enantiomeric structure to the surface layers. Significantly, however, there is little distortion of CdS geometry in the QD core.

We have therefore tested the three proposed models[14] for circular dichroism in a QD with chiral ligands: (i) the core of the QD is chiral; (ii) the QD surface is chiral; (iii) only the adsorbate is chiral. Our experimental and theoretical results support model (ii).

Acknowledgment. We thank the SFI-funded National Access Programme for access to modeling capabilities at Tyndall National Institute. We also thank SFI and CRANN Institute for their financial support and the Department of Materials, University of Oxford, and the European Community for access to HRTEM via the ESTEEM project (contract no. 026019).

Supporting Information Available: DFT optimized coordinates in *xyz* format. This material is available free of charge via the Internet at http://pubs.acs.org.

References

(1) Bruchez, M., Jr.; Moronne, M.; Gin, P.; Weiss, S.; Alivisatos, A. P. *Science* **1998**, *281*, 2013–2016.
(2) Gaponik, N.; Talapin, D. V.; Rogach, A. L.; Hoppe, K.; Shevchenko, E. V.; Kornowski, A.; Eychmuller, A.; Weller, H. *J. Phys. Chem. B* **2002**, *106*, 7177–7185.
(3) Alivisatos, P. *Nat. Biotechnol.* **2004**, *22*, 47–52.
(4) Jovin, T. M. *Nat. Biotechnol.* **2004**, *21*, 32–33.
(5) Empedocles, S.; Bawendi, M. *Acc. Chem. Res.* **1999**, *32*, 389–396.
(6) Afzaal, M.; O'Brien, P. J. *Mater. Chem.* **2006**, *17*, 1597–1602.
(7) Nirmal, M.; Brus, L. *Acc. Chem. Res.* **1999**, *32*, 407–414.
(8) Schill, A. W.; Gaddis, C. S.; Qian, W.; El-Sayed, M. A.; Cai, Y.; Milam, V. T.; Sandhage, K. *Nano Lett.* **2006**, *6*, 1940–1949.
(9) Byrne, S. J.; Corr, S. A.; Rakovich, T. Y.; Gun'ko, Y. K.; Rakovich, Y. P.; Donegan, J. F.; Mitchell, S.; Volkov, Y. *J. Mater. Chem.* **2006**, *16*, 2896–2902.
(10) Michalet, X.; Pinaud, F. F.; Bentolila, L. A.; Tsay, J. M.; Doose, S.; Li, J. J.; Sundaresan, G.; Wu, A. M.; Gambhir, S. S.; Weiss, S. *Science* **2005**, *307*, 538–544.
(11) Medintz, I.; Uyeda, H.; Goldman, E.; Mattoussi, H. *Nat. Mater.* **2005**, *4*, 435–446.
(12) Wang, S. P.; Mamedova, H.; Kotov, N. A.; Chen, W.; Studer, J. *Nano Lett.* **2002**, *2*, 817–822.
(13) Yao, H.; Miki, K.; Nishida, N.; Sasaki, A.; Kimura, K. J. *J. Am. Chem. Soc.* **2005**, *127*, 15536–15543.
(14) Schaaff, T. G.; Whetten, R. L. *J. Phys. Chem. B* **2000**, *104*, 2630–2641.
(15) Li, T.; Park, H. G.; Lee, H.-S.; Choi, S.-H. *Nanotechnology* **2004**, *15*, S660–S663.
(16) Shemer, G.; Krichevski, O.; Markovich, G.; Molotsky, T.; Lubitz, I.; Kotlyar, A. B. *J. Am. Chem. Soc.* **2006**, *128*, 11006–11007.
(17) Moloney, M. P.; Gun'ko, Y. K.; Kelly, J. M. *Chem. Commun.* **2007**, *2007*, 3900–3902.
(18) Avdeef, A.; Kearney, D. L. *J. Am. Chem. Soc.* **1982**, *104*, 7212.
(19) Gulseren, O.; Ercolessi, F.; Tosatti, E. *Phys. Rev. Lett.* **1998**, *80*, 3775.
(20) Herron, N.; Calabrese, J. C.; Farneth, W. E.; Wang, Y. *Science* **1993**, *259*, 1426–1428.
(21) Vossmeyer, T.; Reck, G.; Schulz, B.; Katsikas, L.; Weller, H. *J. Am. Chem. Soc.* **1995**, *117*, 12881–12882.
(22) TURBOMOLE, University of Karlsruhe . Ahlrichs, R.; Bär, M.; Häser, M.; Horn, H.; Kölmel, C. *Chem. Phys. Lett.* **1989**, 162–165; http://www.turbomole.com.
(23) Becke, A. D. *Phys. Rev. A* **1988**, *38*, 3098. Perdew, J. P. *Phys. Rev. B* **1986**, *33*, 8822.
(24) Eichkorn, K.; Treutler, O.; Oehm, H.; Häser, M.; Ahlrichs, R. *Chem. Phys. Lett.* **1995**, *242*, 652. Eichkorn, K.; Weigend, F.; Treutler, O.; Ahlrichs, R. *Theor. Chem. Acc.* **1997**, *97*, 119. Sierka, M.; Hogekamp, A.; Ahlrichs, R. *J. Chem. Phys.* **2003**, *118*, 9136.
(25) Schäfer, A.; Horn, H.; Ahlrichs, R. *J. Chem. Phys.* **1992**, *97*, 2571.
(26) Andrae, D.; Häussermann, U.; Dolg, M.; Stoll, H.; Preuss, H. *Theor. Chim. Acta* **1990**, *77*, 123.
(27) Frenzel, J.; Joswig, J. O.; Sarkar, P.; Seifert, G.; Springborg, M. *Eur. J. Inorg. Chem.* **2005**, *18*, 3585–3596.
(28) Deglmann, P.; Ahlrichs, R.; Tsereteli, K. *J. Chem. Phys.* **2002**, *116*, 1585.
(29) Moore, G. E., Jr.; Klein, M. V. *Phys. Rev.* **1969**, *179*, 722.
(30) Sanville, E.; Burnin, A.; BelBruno, J. J. *J. Phys. Chem. A* **2006**, *110*, 2378–2386.
(31) We obtain a chemically unreasonable electronic structure when $-COO^-$ is "dangling", i.e., neither coordinated to Cd nor H-bonded to another Pen, as occurs when $-COO^-$ project out over the corners between two faces of the cluster. This may be an artifact of the sharp corners and high curvature of our small cluster geometries. We therefore saturate these corner groups with H^+ (i.e.,$-$COOH, denoted PenH), and this gives a marked improvement in the electronic structure.
(32) The outermost CdS layers are distorted out of C_3 symmetry in response to the localization of highest occupied MOs at individual cluster corners.

NL801453G